Ferroelectric–domain and surface nano-engineering of a near-stoichiometric $LiNbO_3$ single crystal

K. Terabe*, M. Nakamura, S. Takekawa, and K. Kitamura, National Institute for Materials Science, Japan;
S. Higuchi, T. Togashi, Department of Materials Science and Technology, Tokyo University of Tokyo, Japan

Abstract

The ferroelectric domain and surface of single crystal $LiNbO_3$ at the microscale to nanoscale level were engineered and observed by scanning force microscopy (SFM). We used a near-stoichiometric $LiNbO_3$ crystal, that had a coercive field of about one-ninth that of a conventional congruent $LiNbO_3$ crystal, as the sample. The z-cut $LiNbO_3$ crystals fixed on metal substrates were polished to a thickness of approximately 5 μm. Domain structures were patterned in the samples with SFM, where the domains were inverted by scanning with the conductive cantilever while applying appropriate voltages. We also preferentially etched the negatively polarized surfaces of the domains in the patterns in a 1:2 mixture of HF and HNO_3 acid solutions. As a result, surface morphologies with patterned structures, such as mound-array, were fabricated and these engineered structures in $LiNbO_3$ crystals could be used in the future to create additional unique (smart) templates and devices.

Introduction

Lithium niobate ($LiNbO_3$: LN, hereafter) is a ferroelectric material that has superior electro-optical, nonlinear-optical, piezoelectric and pyroelectric properties. Therefore, it is an attractive functional material for potential use in light-wavelength-conversion, light-modulation, hologram-memory and micro-electromechanical-system (MEMS) devices. In some of these, ferroelectric domain structures are artificially fabricated in the crystal, leading to induce functions. For example, second harmonic generation (SHG) [1] and optical parametric oscillation (OPO) [2] devices have been fabricated by utilizing quasi phase matching (QPM) [3], which is induced by the formation of periodically poled domain structures at the microscale level. Thus, the availability of technology to arbitrarily fabricate domain structures, such as gratings, in crystal is one of the most important factors affecting the development of optical devices and MEMS. In addition, the availability of technology that allows us to arbitrarily fabricate surface morphology is also important in helping us develop these functional devices. However, in contrast with semiconductor device processing, there are few appropriate means of engineering the surface morphology of LN crystals through physical etching techniques. Surface engineering at the microscale level was recently demonstrated through a chemical etching technique, where domain inversion was done in a LN crystal using photolithographic patterning followed by electric field poling. The negatively polarized surfaces of the domains in the pattern were preferentially etched in a mixture of HF and HNO_3 acids [4, 5].

We have investigated the microscale to nanoscale domain engineering of ferroelectric crystals through scanning force microscopy (SFM) [6-8], which enables the polarization of ferroelectric domains to be inverted at the submicroscale and even nanoscale level [9-14]. It also enables noninvasive observation of inverted domain structures. The development of a technology to engineer domain and surface structures at the submicroscale and nanoscale level will not only improve functions in conventional devices, but will also promote the creation of additional unique (smart) templates and devices. In this study, we investigated the possibilities of constructing patterned domain structures within the LN crystal with SFM and of processing the surface morphology by preferential etching, thereby making use of the difference in the polarity of polarized faces in the domain patterns.

Report Documentation Page

Form Approved
OMB No. 0704-0188

1. REPORT DATE	2. REPORT TYPE	3. DATES COVERED
00 JUN 2003	**N/A**	**-**

4. TITLE AND SUBTITLE	5a. CONTRACT NUMBER
Ferroelectricdomain and surface nano-engineering of a near-stoichiometric LiNbO3 single crystal	5b. GRANT NUMBER
	5c. PROGRAM ELEMENT NUMBER
6. AUTHOR(S)	5d. PROJECT NUMBER
	5e. TASK NUMBER
	5f. WORK UNIT NUMBER
7. PERFORMING ORGANIZATION NAME(S) AND ADDRESS(ES) **National Institute for Materials Science, Japan; Department of Materials Science and Technology, Tokyo University of Tokyo, Japan**	8. PERFORMING ORGANIZATION REPORT NUMBER
9. SPONSORING/MONITORING AGENCY NAME(S) AND ADDRESS(ES)	10. SPONSOR/MONITOR'S ACRONYM(S)
	11. SPONSOR/MONITOR'S REPORT NUMBER(S)

12. DISTRIBUTION/AVAILABILITY STATEMENT
Approved for public release, distribution unlimited

13. SUPPLEMENTARY NOTES
See also ADM001697, ARO-44924.1-EG-CF, International Conference on Intelligent Materials (5th) (Smart Systems & Nanotechnology)., The original document contains color images.

14. ABSTRACT

15. SUBJECT TERMS

16. SECURITY CLASSIFICATION OF:			17. LIMITATION OF ABSTRACT	18. NUMBER OF PAGES	19a. NAME OF RESPONSIBLE PERSON
a. REPORT	b. ABSTRACT	c. THIS PAGE			
unclassified	**unclassified**	**unclassified**	**UU**	**7**	

Materials and experimental method

We used a bulky single crystal of LN as the material for the domain and surface engineering, because we thought that the structural non-uniformity in the current LN thin film prepared by vapor deposition methods would probably create serious problems at the nanoscale level. A single crystal of near-stoichiometric LN (with 1% MgO doping) was grown with a new double-crucible Czochralski method, that we developed, that had an automatic powder supply system [15]. There is a photograph of the clear LN single crystal in Fig. 1(a). Compared to a LN single crystal obtained with the conventional Czochralski method using congruent melt, the LN single crystal obtained with our new method had a composition close to stoichiometric (Li/Nb=1). Therefore, there were an extremely small number of nonstoichiometric defects in the crystal and this contributed to superior optical properties [16-18]. Furthermore, the coercive field (electric field to switch polarization of ferroelectric domain) was found to have decreased drastically [19]. A ferroelectric hysteresis loop of the LN crystal was obtained by conventional measurement using liquid electrodes 4 mm in diameter (LiCl solution in water) at room temperature (Fig. 1(b)). The hysteresis loop indicates that the polarization of the domains can be inverted homogeneously by applying an appropriate electric field and the coercive field is approximately 2.3 kV/mm. The coercive field is about one-ninth that of an LN crystal obtained by the conventional Czochralski method using congruent melt. The decrease in the coercive field is extremely advantageous in domain engineering with SFM, because polarization inversion is possible with a relatively low applied voltage.

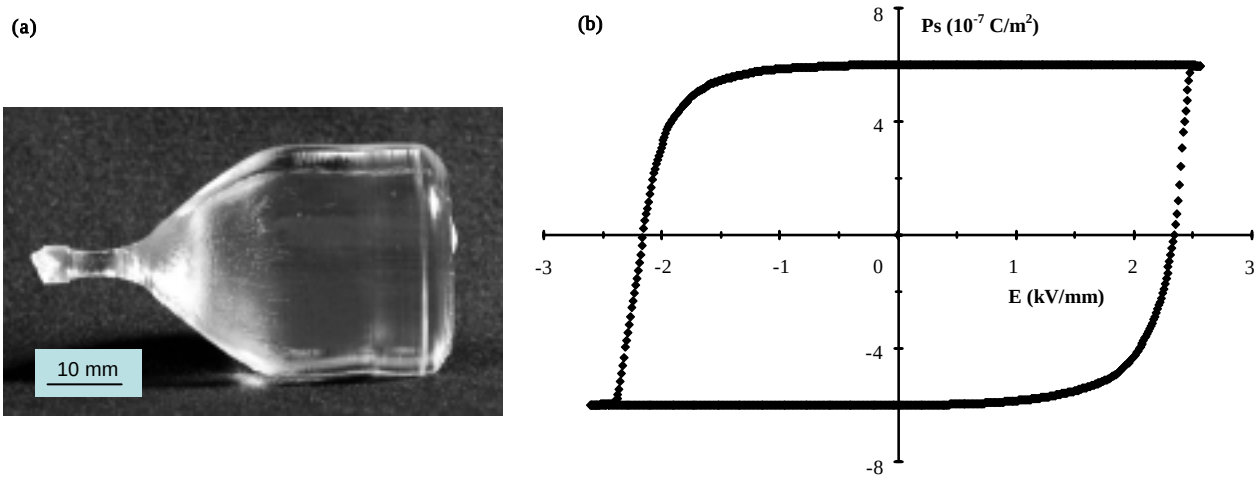

Figure 1: (a) Photograph of near-stoichiometric LN single crystal (with 1% MgO doping) grown by double-crucible Czochralski method with automatic powder supply system (b) and ferroelectric hysteresis loop of LN crystal obtained at room temperature by conventional measurement using liquid electrodes.

The LN single crystal, which has a single 180°-domain structure (polarization is parallel to z-axis), was cut perpendicular to the z-axis. Gold films were deposited on one side of the cut plate-crystals and the surfaces covered with these were attached onto metal substrates using conductive paste. The crystals on the metal substrates were polished to approximately 5 μm. The domain inversion of the LN samples, as we can see from Fig. 2, was achieved by applying an appropriate dc bias voltage between the conductive cantilevers and metal substrates, where the latter were grounded. We used conductive SFM cantilevers made of tetrahedral silicon tips with a radius of less than 25 nm, which were coated with platinum/titanium metals. The resonance frequency and spring constant were 70 kHz and 2 N/m. The tailored patterns of the inverted domain structures were fabricated by scanning the samples with the conductive cantilevers while applying appropriate voltages. The piezoresponse mode of the SFM was expected to be able to directly image the domain structures at nanoscale resolution. We imaged the fabricated patterns of the inverted structures in this mode.

We investigated the etching properties of the LN crystal at submicroscale to nanoscale levels with SFM. The z-cut LN crystals, which had anti-parallel polarization of domains, were etched in various mixtures of HF and HNO_3 acids for different periods at 20 °C. Figure 3 has an example of the topography of surface morphology after etching in 1:2 mixture of HF and HNO_3 acids for 1500 s. The negatively polarized surface (represented by –z-face) of the domain was preferentially etched. The etching rate was determined by measuring the etch depth of the –z-face. The LN samples subjected to domain patterning with SFM were etched using 1:2 mixture of HF and HNO_3 acids, and the surface morphologies after etching were observed in the SFM topographic mode.

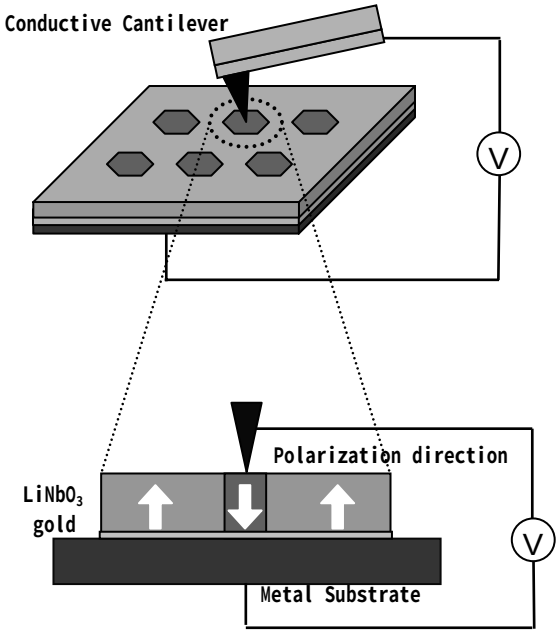

Figure 2: Domain engineering method using SFM. Polarizations of ferroelectric domains in LN crystal were locally switched by applying bias voltage using conductive cantilever.

Domain engineering

We examined the shapes of inverted domains in LN samples under different bias voltages and over different periods of time. Figure 4 shows the shapes of domains inverted by applying voltage V = -40 V for treatment times ranging from 1 to 4800 s. The inverted domains in the figure are hexagonal (represented by black areas); the shape originates from the LN crystal structure. As the treatment times increased, the domains grew from approximately 500 nm to 3.5 μm. As the polarizations of these inverted domains are directed from the bottom of the crystal to the surface; the domain surfaces are positively polarized (+z-face). In addition, when the treatment time was fixed at 120 s, the inverted domains grew lineally from 500 nm to 2.6 μm as the voltage increased from 17.5 to -60 V. Figure 5(a) shows the relationship between domain size and treatment time, and Fig. 5(b) that between domain size and bias voltage. These indicate that inverted domains of arbitrary size can be fabricated with SFM by controlling the bias voltage and treatment time. When treatment time was decreased to less than 1 s, a domain size of less than 500 nm was fabricated; however, this domain disappeared with time. Yet, when an LN sample polished to a thickness of approximately 3 μm was used, the resulting inverted domain of approximately 300 nm did not disappear over time. This may have been because when a 5-μm-thick LN sample was used the domain could not grow penetrating through from the bottom to the surface; i.e., the domain structure was unstable in terms of electrostatic energy. Recently, Cho *et al.* demonstrated that stable inverted-domains of 28 nm or less than one were formed in $LiTaO_3$ single crystals when crystals thinned to approximately 100-nm thickness by dry etching were used [20].

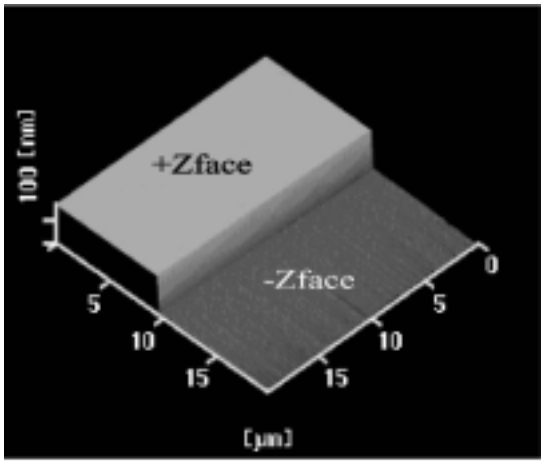

Figure 3: SFM stereo-topographic micrograph of surface morphology after etching. Sample of z-cut LN crystal, which has anti-parallel polarization of domains, was etched in a 1:2 mixture of HF and HNO_3 acids for 1500 s at 20 °C.

We fabricated inverted domain structures with tailored patterns by scanning with a conductive cantilever on the LN samples while applying the appropriate voltage. Figures 6 and 7 have examples of fabricated domain structures with a linear pattern and a dot-array pattern, respectively. The linear pattern of the inverted domain (represented by black area)

was fabricated by scanning the sample with the cantilever at the rate of 500 nm/s, while applying a voltage of V= -60 V. The width of the linear inverted-domain in the pattern was approximately 500 nm. The dot-array pattern, on the other hand, was fabricated by scanning the sample with the cantilever, while applying a voltage of V= -60 V on it repeatedly at 1 s intervals. The size of the dotty inverted-domain in the pattern was approximately 600 nm.

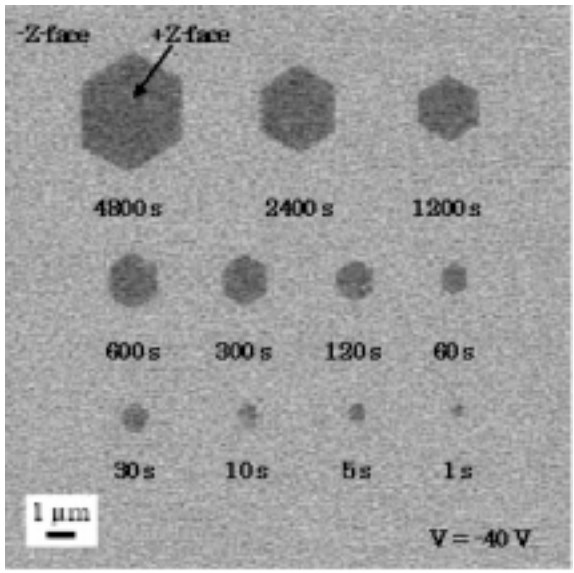

Figure 4: SFM piezoresponse micrograph of ferroelectric domains inverted by applying bias voltage of V= -40 V for various treatment times. Black and grey areas correspond to +z- and –z-faces of polarized domain.

Surface engineering

We know that the –z-face is preferentially etched when an LN crystal that is cut perpendicular to the z axis (with a 180° domain) is immersed in a mixture of HF and HNO_3 acid solutions [4, 5, 21]. We investigated the etching properties of the LN crystal, such as etch rate and etched surface morphology, with SFM to establish the appropriate conditions for nanoscale surface engineering. LN crystals with anti-parallel polarizations in domains were etched in (1:0, 1:1, 1:2, and 0:1) mixtures of HF and HNO_3 acids from 60 to 2400 s at 20 °C. SFM observation in the topographic mode (for example, Fig. 3) revealed that the –z-face of the domain was etched in 1:2 mixture, but absolutely no etching occurred on the +z-face. The step formed by etching, at the boundary of +z- and –z-faces, was very sharp. The etch rate of–z faces was determined by measuring the etch depth. Figure 8 shows the relationship between the etch depth and the treatment times in these mixtures. The etch depth in (1:0, 1:1, and 1:2) mixtures increased lineally as the treatment times increased; but absolutely no etching occurred in the 0:1 mixture (pure HNO_3). The etch rate in (1:0, 1:1, and 1:2) mixtures of HF and HNO_3 decreased as the HNO_3 concentration increased. The etching rate in the 1:2 mixture was 1/3 faster than that in the 1:0 mixture (pure HF). This indicates that the etch depth can be controlled at submicroscale to nanoscale levels by changing the treatment time and HNO_3 concentration of the mixture. We also examined the roughness of the etched surface with SFM imaging. Figure 9 (a) has topographic micrographs of surfaces morphologies formed by etching in

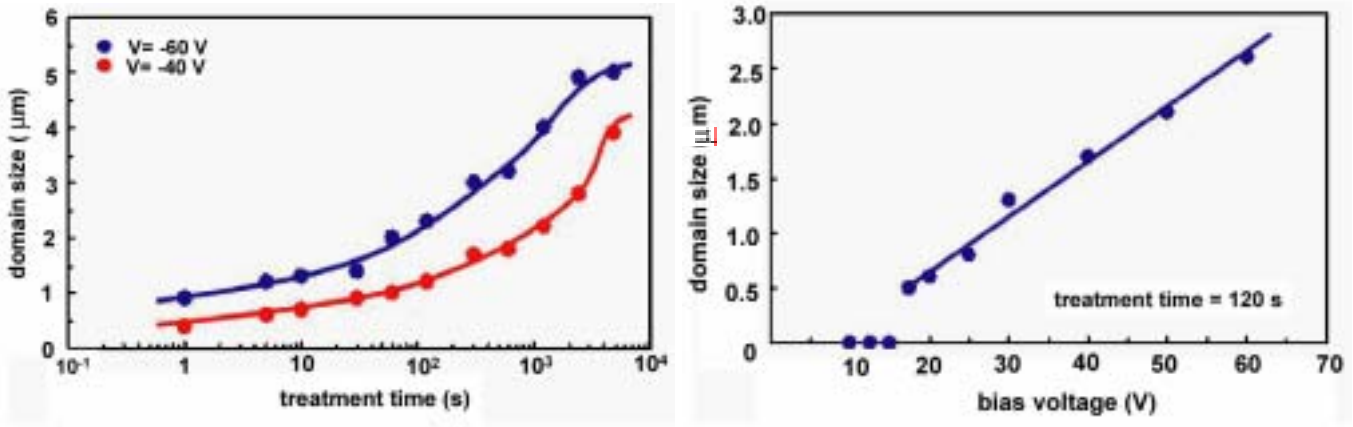

Figure 5: (a) Relationship between domain size and treatment time with bias voltage of V = -40 and V = -60 V and (b) relationship between domain size and bias voltage with treatment time of 120 s.

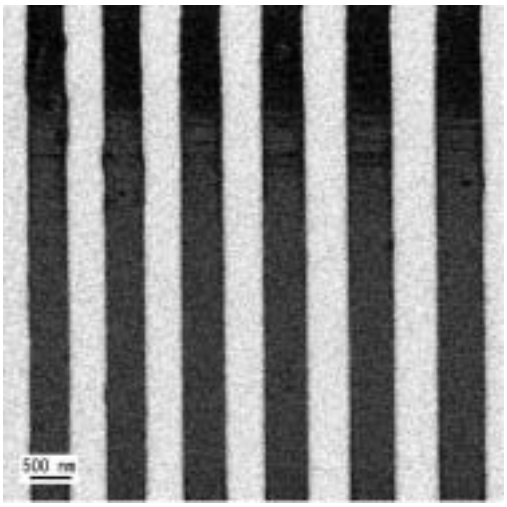

Figure 6: SFM piezorespose micrographof linear pattern made up of inverted-domains

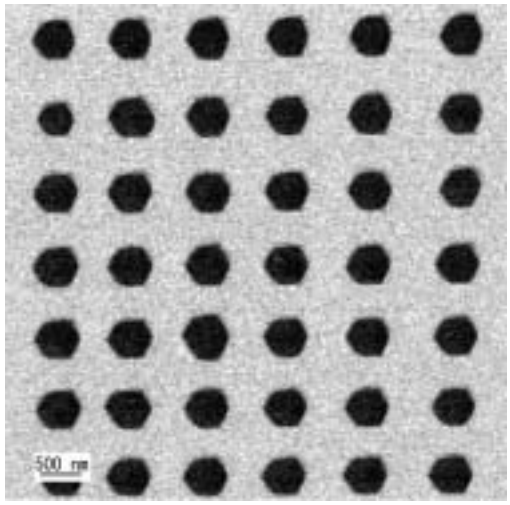

Figure 7: SFM piezorespose micrographof dot-array pattern made up of dotty inverted-domains

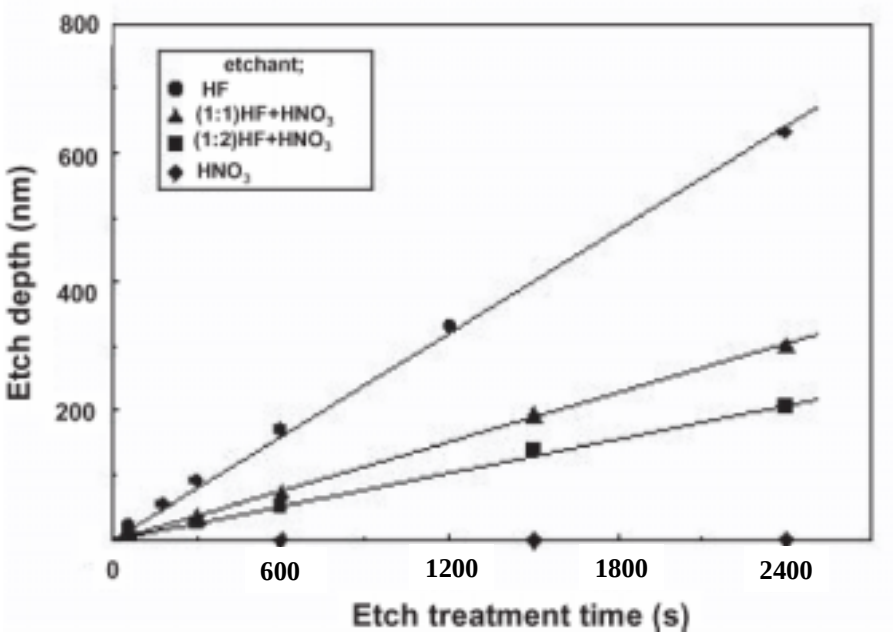

Figure 8: Relationship between etch depth and treatment time in (1:0, 1:1, 1:2, and 1:0) mixtures of HF and HNO_3 acids at 20 °C.

1:2 mixture for 2400 s. The etch depth of the sample was approximately 200 nm. The peak-to-peak roughness of the etched surface was approximately 9 nm. These indicate that the etching rate was slow and the etched surface with very smooth morphology was obtained when 1:2 mixture was used. We consider this mixture is appropriate etchant for nano-engineering the LN surface because the control of etch depth is easy at the nanoscale level.

We etched the LN sample with a patterned domain structure (which is shown in Fig. 7) using the 1:2 mixture. If the LN sample attached onto metal substrate using conductive paste is immersed in a mixture of HF and HNO_3 acid solutions, the metal substrate and the paste is damaged. Thus, the sample was etched by dripping one drop of the mixture onto the surface and keeping it there for 3600 sec. Figure 10 is a topographic micrograph that represents the sample surface morphology after etching. The –z-face (gray area in Fig. 7) was etched, but the +z-face (black area) was

not. As a result, mound-array structure with a radius of 600 nm and a height of 80 nm was fabricated. The etch rate slowed down in comparison with the case (Fig. 8) in which the sample was immersed in the mixture. The radii of

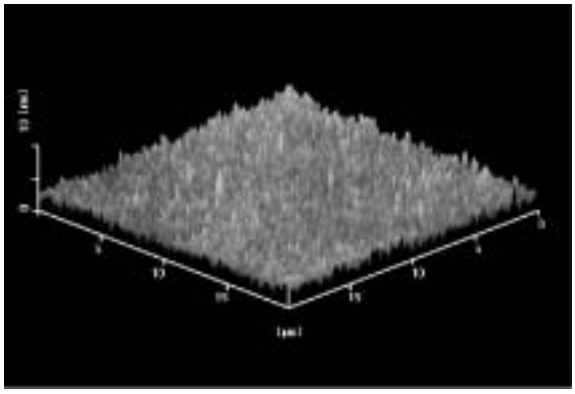

Figure 9: (a) SFM stereo-topographic micrograph of LN surfaces etched in 1:2 mixture of HF and HNO_3 acids for 2400 s.

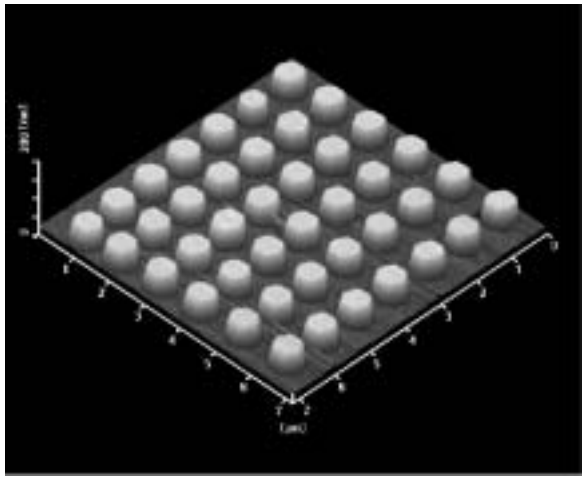

Figure 10 SFM stereo-topographic micrograph of mound-array pattern of surface morphology formed by preferentially etching in 1:2 mixure of HF and HNO_3 acids for 3600 s.

mounds precisely matched those of the inverted domain dots (Fig. 7). In contrast, when the domain structure was fabricated so that the dotted regions represented the –z-face, a surface structure with a cavity-array pattern was fabricated [7].

Conclusion

We investigated the microscale to nanoscale engineering of the ferroelectric domain structure and surface morphology of a near-stoichiometric LN single crystal with SFM. We were able to fabricate domain structures with tailored patterns by controlling the magnitude of the bias voltage, polarity, and treatment time applied to LN samples while scanning them with the conductive cantilever. In addition, we could fabricate surface morphologies with tailored shapes on the LN samples by preferentially etching the negatively polarized face in the patterned domains using a 1:2 mixture of HF and HNO_3 acids. We believe that domain and surface engineering have great potential in the development of additional unique (smart) templates, NEMS, and optical devices; i.e., photonic crystals with optical properties controlled by externally applying voltage, light, or pressure could be created.

Reference

[1] K. Yamamoto, K. Mizuuchi, K. Takeshige, Y. Sasai, and T. Taniuchi, “Characteristics of periodically domain- inverted $LiNbO_3$ and $LiTaO_3$ waveguides for second harmonic generation”, *J. Appl. Phys.*, **70**, 1947-1951, 1991.

[2] R. W. Wallance, “Stable, efficient, optical parametric oscillators pumped with doubled Nd: YAG”, *Appl. Phys. Lett.*, **17**, 497-499, 1970.

[3] J. A. Armstrong, N. Bloembergen, J. Ducuing, and P. S. Pershan, “Integrations between light waves in a nonlinear dielectric”, *Phys. Rev.*, **127**, 1918-1939, 1962.

[4] I. E. Barry, G. W. Ross, P. G. R. Smith, R. W. Eason, and G. Cook, “Microstructuring of lithium niobate using differential each-rate between inverted and non-inverted ferroelectric domain”, *Mater. Lett.* **37**, 246-254, 1998

[5] C. L. Sones, S. K. Mailis, W. S. Brocklesby, R. W. Eason, and J. R. Owen, “Differential eatch rates in z-cut LiNbO3 for variable

HF/HNO3 concentration", *J. Mater. Chem*. **12**, 295-298, 2002

[6] K. Terabe, S. Takekawa, M. Nakamura, K. Kitamura, S. Higuchi, Y. Gotoh, and A. Gruverman, "Imaging and engineering the nanoscale-doamin structure of a $Sr_{0.61}Ba_{0.39}Nb_2O_6$ crystal using a scanning force microscope", *Appl. Phys. Lett.*, **81**, 2044-2046, 2002.

[7] K. Terabe, M. Nakamura, S. Takekawa, K. Kitamura, S. Higuchi, Y. Gotoh, and Y. Cho, "Microscale to nanoscale ferroelectric domain and surface engineering of a near-stoichiometric $LiNbO_3$ crystal", *Appl. Phys. Lett.*, **82**, 433-435, 2003

[8] K. Terabe, S. Higuchi, S. Takekawa, M. Nakamura, Y. Gotoh, and K. Kitamura, "Nanoscale domain engineering of $Sr_{0.61}Ba_{0.39}Nb_2O_6$ single crystal using a scanning force microscope", *Ferroelectrics*, in press

[9] A. Gruverman, O. Auciello, and H. Tokumoto, "Nanoscale investigation of fatigue effects in $Pb(Zr,Ti)O_3$ films" *Appl. Phys. Lett.*, **69**, 3191-3193, 1996.

[10] Y. G. Wang, W. Kleemann, T. Woike, and R. Pankrath, "Atomic force microscopy of domains and volume holograms in $Sr_{0.61}Ba_{0.39}Nb_2O_6:Ce^{3+}$", *Phys. Rev. B*, **61**, 3333-3336, 2000.

[11] A. Gruverman, O. Auciello, J. Hatano, and H. Tokumoto, "Scanning force microscopy as a tool for nanoscale study of ferroelectric domains", *Ferroelectrics*, **184**, 11-20, 1996.

[12] S. Kazuta, Y. Cho, H. Odagawa, and K. Kitamura, "Small inverted domain formation in stoichiometric $LiTaO_3$ single crystal using scanning nonlinear dielectric microscopy", *Integrated Ferroelectrics*, **38**, 49-57, 2001.

[13] L. M. Eng, "Nanoscale domain engineering and characterization of ferroelectric domains", *Nanotechnology*, **10**, 405-411, 1999

[14] P. Paruch, T. Tybell, and J.-M. Triscone, "Nanoscale control of ferroelectric polarization and domain size in epitaxial $Pb(Zr_{0.2}Ti_{0.8})O_3$ this film", *Appl. Phys. Lett*, **23**, 530-532, 2001

[15] K. Kitamura, J. K. Yamamoto, N. Iyi, S. Kimura, and T. Hayashi, "Stoichiometric $LiNbO_3$ single crystal growth by double crucible Czochralski method using automatic powder supply system", *J. Cryst.Growth***, 116,** 327-332**,** 1992

[16] K. Kitamura, Y. Furukawa, Y. Ji, M. Zgonik, C. Medrano, G.. Montemezzani, and P. Gunter, "Photorefractive effect in $LiNbO_3$ crystals enhanced by stoichiometry control", *J. Appl. Phys*. **82,** 1006-1009, 1997

[17] T. Fujiwara, M. Takahashi, M. Ohma, A. Ikushima, Y. Furukawa, and K. Kitamura, Comparison of electro-optic effect between stoichiometric and congruent $LiNbO_3$, *Electron Lett.* **35**, 499-501, 1999

[18] M. Nakamura, S. Higuchi, S. Takekawa, K. Terabe, Y. Furukawa, and K. Kitamura, "Optical Damage Resistance and Refractive Indices in Near-Stoichiometric MgO-Doped $LiNbO_3$", J*pn. J. Appl. Phys*. **41**, L49-51, 2002

[19] V. Gopalan, T. E. Mitchell, Y. Furukawa, and K. Kitamura, "The role of nonstoichiometry in 180° domain switching of $LiNbO_3$ crystal", *Appl. Phys. Lett.* **72**, 1981-1983, 1998

[20] Y. Cho, K. Fujimoto, Y. Hiranaga, Y, Wagatsuma, A Onoe, K. Terabe, and K. Kitamura, "Tbit/inch^2 ferroelectric data storage based on scanning nonlinear dielectric microscopy", *Appl. Phys. Lett.* **81**, 4401-4403, 2002

[21] S. Miyazawa, "Ferroelectric domain inversion in Ti-diffused $LiNbO_3$ optical waveguide", *J. Appl. Phys.* **50**, 4599-4603, 1979